EMBO reports

scientific report

Subunit architecture of multimeric complexes isolated directly from cells

Helena Hernández[1], Andrzej Dziembowski[2]*, Thomas Taverner[1], Bertrand Séraphin[2+] & Carol V. Robinson[1++]*

[1]Department of Chemistry, University of Cambridge, Cambridge, UK, and [2]Équipe labelisée 'La Ligue', CGM-CNRS, Gif sur Yvette, France

Recent developments in purification strategies, together with mass spectrometry (MS)-based proteomics, have identified numerous *in vivo* protein complexes and suggest the existence of many others. Standard proteomics techniques are, however, unable to describe the overall stoichiometry, subunit interactions and organization of these assemblies, because many are heterogeneous, are present at relatively low cellular abundance and are frequently difficult to isolate. We combine two existing methodologies to tackle these challenges: tandem affinity purification to isolate sufficient quantities of highly pure native complexes, and MS of the intact assemblies and subcomplexes to determine their structural organization. We optimized our protocol with two protein assemblies from *Saccharomyces cerevisiae* (scavenger decapping and nuclear cap-binding complexes), establishing subunit stoichiometry and identifying substoichiometric binding. We then targeted the yeast exosome, a nuclease with ten different subunits, and found that by generating subcomplexes, a three-dimensional interaction map could be derived, demonstrating the utility of our approach for large, heterogeneous cellular complexes.

Keywords: mass spectrometry; tandem affinity purification; exosome; scavenger decapping complex; cap-binding complex

EMBO reports (2006) **7**, 605–610. doi:10.1038/sj.embor.7400702

INTRODUCTION

Several important cellular functions require the activities of large cellular machines composed of protein subunits, which are often associated with nucleic acid components or other cofactors. High-throughput proteomic approaches have allowed a tantalizing glimpse of many complexes predicted from extensive protein interaction networks, creating a need for new methodologies to provide insights into the organization of protein subunits in both homogeneous and heterogeneous complexes at natural expression levels. Our rationale for combining tandem affinity purification (TAP) with nanoflow electrospray mass spectrometry (MS) is based on selectivity and direct detection of interacting subunits. Selectivity is achieved in a single TAP isolation, which involves using an engineered subunit of the proposed complex, the 'target' protein, with two separate affinity tags for a two-stage purification strategy. This process preserves all interaction partners of the target protein under natural assembly parameters and greatly reduces the possibility of nonspecific interactions; the TAP procedure has been widely applied for large-scale proteomic analyses (Gavin *et al*, 2002, 2006) and many TAP-tagged complexes have been characterized extensively (Rigaut *et al*, 1999; Bushnell & Kornberg, 2003). For direct detection of these TAP-tagged complexes, we used methods designed to maintain non-covalent complexes within the mass spectrometer (Sobott & Robinson, 2002) to provide definitive evidence for stoichiometric complexes, in which all subunits are present in equivalent ratios, and generated subcomplexes by perturbation both in solution and in gas phases. The overlap between the subcomplexes can then be used to construct an interaction map.

[1]Department of Chemistry, University of Cambridge, Lensfield Road, Cambridge CB2 1EW, UK
[2]Équipe labelisée 'La Ligue', CGM-CNRS, Avenue de la Terrasse, 91198 Gif sur Yvette Cedex, France
*These authors contributed equally to this work
[+]Corresponding author. Tel: +33 169 823 883; Fax: +33 169 823 877;
E-mail: bertrand.seraphin@cgm.cnrs-gif.fr
[++]Corresponding author. Tel: +44 1223 763 846; Fax: +44 1223 336 362;
E-mail: cvr24@cam.ac.uk

Received 6 February 2006; revised 5 April 2006; accepted 7 April 2006; published online 19 May 2006

RESULTS AND DISCUSSION

Composition of dimeric and trimeric complexes

We explored the composition of buffers for purification and concentration, and determined strategies compatible with electrospray ionization (ESI) analysis of TAP complexes (see Methods; supplementary information online). Using these approaches, we purified the scavenger decapping complex responsible for the degradation of the messenger RNA cap released during mRNA decay (Wang & Kiledjian, 2001; Liu *et al*, 2002). This complex is present at about 10,000 copies per cell at the late growing phase (Ghaemmaghami *et al*, 2003; Malys *et al*, 2004). We used a Dcs2 TAP fusion and, after optimization of the TAP protocol, mass spectra showed only one principal species, consistent with the heterodimer Dcs1:Dcs2-CBP, where CBP refers to the tag remaining after cleavage with the tobacco etch virus protease (Fig 1A; supplementary Table 2 online); no other complexes or components were evident. To validate the composition of the

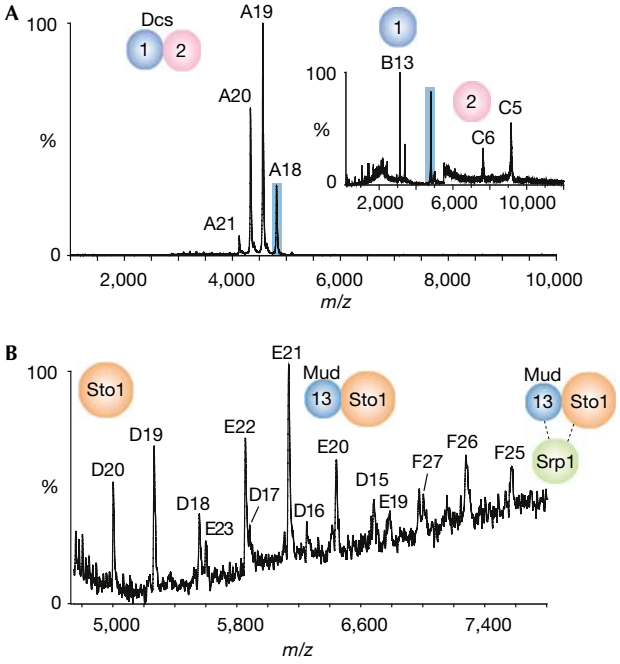

Fig 1 | MS of intact dimeric and trimeric complexes. (**A**) MS of the scavenger decapping complex shows only one principal species, with charge states labelled A18–A21, consistent with a heterodimer of Dcs1 and Dcs2-CBP. Inset: MS/MS spectrum obtained after isolation and dissociation of the 18+ charge state highlighted in blue to yield products B and C (Dcs1 and Dcs2-CBP, respectively). (**B**) Nuclear cap-binding complex consisting of Mud13-CBP and Sto1 (series E) illustrating interaction with SRP1 (series F). The dashed lines indicate that Srp1 could be associated with either or both of Mud13-CBP and Sto1. CBP, calmodulin-binding peptide; MS, mass spectrometry.

complex, we carried out tandem MS (MS/MS) experiments and confirmed the composition of the heterodimer.

The second moderately abundant yeast complex (~11,000 copies; Ghaemmaghami *et al*, 2003), the nuclear cap-binding complex (CBC), binds to the cap of pre-mRNAs and mRNAs in the nucleus (Gorlich *et al*, 1996; Lewis *et al*, 1996). It is known to be composed of Sto1 and Mud13 subunits, which interact strongly with yeast importin α, Srp1 (Gorlich *et al*, 1996), responsible for dissociating CBC from mRNA in the cytoplasm and transporting it back to the nucleus. CBC has previously been purified by the TAP method and the resulting material was shown to be active (Rigaut *et al*, 1999). From MS, three main species could be detected (Fig 1B). The largest component is consistent with the trimer Mud13-CBP:Sto1:Srp1. In addition, a dimer Mud13-CBP:Sto1 was detected, as well as Sto1 alone. Our results indicate that yeast CBC is heterodimeric and that a fraction of this complex interacts with Srp1. These findings are consistent with structural data available for human CBC (Mazza *et al*, 2002) and the presence of a single nuclear localization sequence in Sto1 responsible for the interaction with Srp1/importin α (Gorlich *et al*, 1996). The spectrum in Fig 1B highlights one of the significant advantages of this approach, that populations of interacting subunits are readily apparent.

Deriving a protein interaction map for the yeast exosome

Our results with the heterodimer and heterotrimer prompted us to examine a much larger complex of high biological interest: the yeast exosome. This evolutionarily conserved multisubunit complex having 3′→5′ exoribonuclease activity is present in both the nucleus and cytoplasm and is involved in RNA processing and turnover (Mitchell *et al*, 1997; Mitchell & Tollervey, 2000). It is composed of six distinct subunits homologous to the catalytic domains of phosphorolytic bacterial RNase PH and polynucleotide phosphorylase PNPase (Rrp41, Rrp42, Rrp43, Rrp45, Rrp46 and Mtr3), three subunits with RNA-binding motifs (Rrp40, Rrp4 and Csl4) homologous to those found in PNPase and one large subunit (Dis3/Rrp44) belonging to the RNase R family of hydrolytic RNases. We purified the cytoplasmic form of the exosome, initially using two different target proteins, Dis3 and Rrp41. Spectra recorded showed that, in both cases, intact, ten-component complexes could be observed. The spectra also showed another charge state series with a mass consistent with the absence of Csl4, demonstrating that Csl4 is substoichiometric (supplementary Fig 2 online). To reduce this heterogeneity, Csl4 was used as the target protein. In this preparation, the intact, ten-component complex (398 kDa) was the principal species (Fig 2), confirming that it can be isolated intact and presenting us with the formidable challenge of deciphering an interaction map for the ten protein subunits that it contains. To do this, we used three different target proteins to isolate the exosome and generated a series of subcomplexes through partial denaturation and perturbation of the complex.

The first of these subcomplexes were observed under the same solution conditions as the intact complexes. A series of low-intensity peaks were evident below 5,000 *m/z*, several of which can be attributed to individual exosome proteins (Fig 2B). Species of masses 85 kDa and 112 kDa are also apparent (Fig 2B,C); MS/MS of the 85 kDa species yielded products with masses corresponding to individual proteins Rrp46 and Rrp40 and dimers Rrp45:Rrp40 and Rrp45:Rrp46 consistent with the heterotrimer Rrp40:Rrp45:Rrp46 (Fig 2A); the 112 kDa series is assigned to the tetramer Rrp41:Rrp40:Rrp45:Rrp46 (Fig 2C). To probe proteins at the core of the exosome, we used stepwise addition of organic solvents to complex-containing solutions, reasoning that this would disrupt hydrophobic interactions and generate additional subcomplexes. Under relatively high percentages of denaturant (33% dimethylsulphoxide (DMSO)), we found that we could generate in solution three distinct species of 56–68 kDa (Fig 2D). MS/MS confirmed that these are dimeric complexes: Rrp42:Mtr3, Rrp41:Rrp45 and Rrp43:Rrp46. Using the trimer and tetramer deduced above (Rrp41:Rrp40:Rrp45:Rrp46), and assuming that the three dimers form the ring observed for the related bacterial PNPase and RNase PH (Symmons *et al*, 2002), there are two possible orientations for the Rrp42:Mtr3 dimer: with Mtr3 contacting either Rrp43 or Rrp41. To distinguish between these possibilities, we looked for subcomplexes generated in solution in which Mtr3 is lost in conjunction with other ring proteins, reasoning that loss of neighbouring proteins is more likely than losses from different locations, which would split the ring into two. We found two subcomplexes resulting from loss of Csl4:Rrp43 and Csl4:Rrp43:Mtr3, strongly implying that Rrp43 is adjacent to Mtr3. This enabled us to deduce the order Rrp41:Rrp45:Rrp46:Rrp43:Mtr3:Rrp42 for the core of the complex.

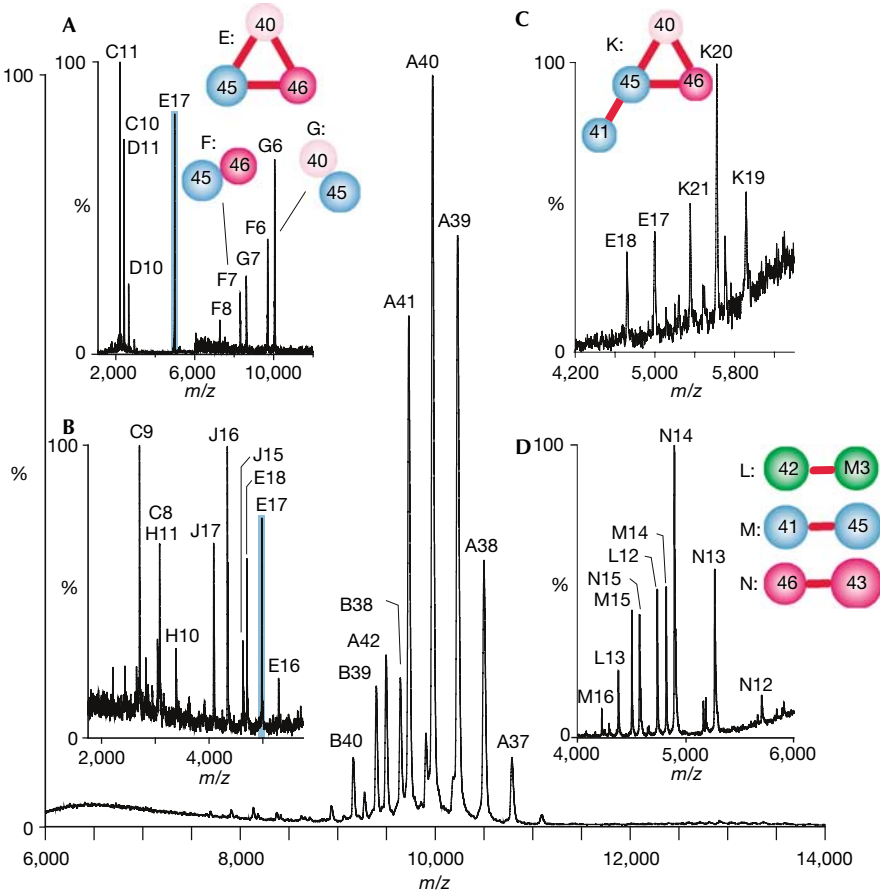

Fig 2 | MS of the intact yeast exosome complex isolated with the Csl4-tagged protein. The main panel shows a charge state series labelled A and B for the intact exosome and complex without Csl4, respectively. (**A**) MS/MS and (**B**) MS spectra of Rrp41-tagged exosome complex, showing the 85 kDa trimer and dissociation products from its 17+ charge state. The dimer and monomer products indicate that the 85 kDa species correspond to the trimer Rrp46:Rrp45:Rrp40. Charge state labels: C Rrp46, D Rrp40, E Rrp45:Rrp40:Rrp46, F Rrp45:Rrp46, G Rrp45:Rrp40, H Rrp45, J yeast heat-shock protein (SSA1/SSA2). (**C**) MS of Dis3-tagged and (**D**) Rrp41-tagged exosome after disruption of the complex in solution using 20% methanol and 33% dimethylsulphoxide, respectively. A heterotetramer K and three different dimers L, M and N are readily identified in the spectra. MS, mass spectrometry.

To define the interactions of Rrp40, Rrp4 and Csl4, we considered solution-phase subcomplexes that contain an incomplete ring together with one or more of these proteins. We found that Rrp40 was observed in only those subcomplexes that contained Rrp45 and Rrp46: the Rrp40:Rrp45 dimer in the MS/MS spectrum confirms the direct interaction of these proteins. The fact that Rrp45 and Rrp46 form two different dimers in the ring strongly implies that Rrp40 bridges these two dimers. We looked for evidence of analogous interactions for Csl4 and Rrp4. In the case of Csl4, no equivalent subcomplex was observed directly, but loss of Rrp43 and Mtr3 is observed when Csl4 is absent, consistent with Csl4's having a role in stabilizing Rrp46:Rrp43 and Mtr3:Rrp42 (Fig 3A). Additionally, a subcomplex generated by collisional activation was observed, corresponding to the loss of Rrp43 from the nine-component complex (intact–Csl4) but not from the intact complex. Taken together, these data indicate that Csl4 bridges dimers Rrp46:Rrp43 and Mtr3:Rrp42. By analogy, internal symmetry suggests that Rrp4 should bridge dimers Rrp41:45 and Rrp42:Mtr3, a proposal strongly supported by the fact that Rrp4 is present in subcomplexes lacking Mtr3, Rrp43 and Rrp46. In summary, Rrp4, Rrp40 and Csl4 have been positioned such that they have key bridging roles between the three ring-forming dimers.

The position of the remaining exosome protein Dis3 could not be determined directly. Dis3 is, however, present in many subcomplexes that lack RNA-binding subunits, indicating that they are not required for the binding of Dis3. The smallest subcomplexes containing Dis3 (Rrp45:Rrp41:Rrp42:Rrp4:Dis3), both with and without Mtr3 (Fig 3), could be generated in either DMSO- or methanol-containing solutions. This indicates that Dis3 interacts with the Rrp45:Rrp41:Rrp42 side of the ring. To explore all possible connections consistent with a data set of common subcomplexes, we used a genetic algorithm to find the shortest path interaction network. The resulting network fully supports our conclusion that Dis3 interacts with one or more of Rrp45, Rrp41 and Rrp42 (Fig 3). Moreover, given the fact that Dis3 is the largest of the exosome proteins (114 kDa), it is reasonable to assume that it is capable of interacting with all three of these ring proteins

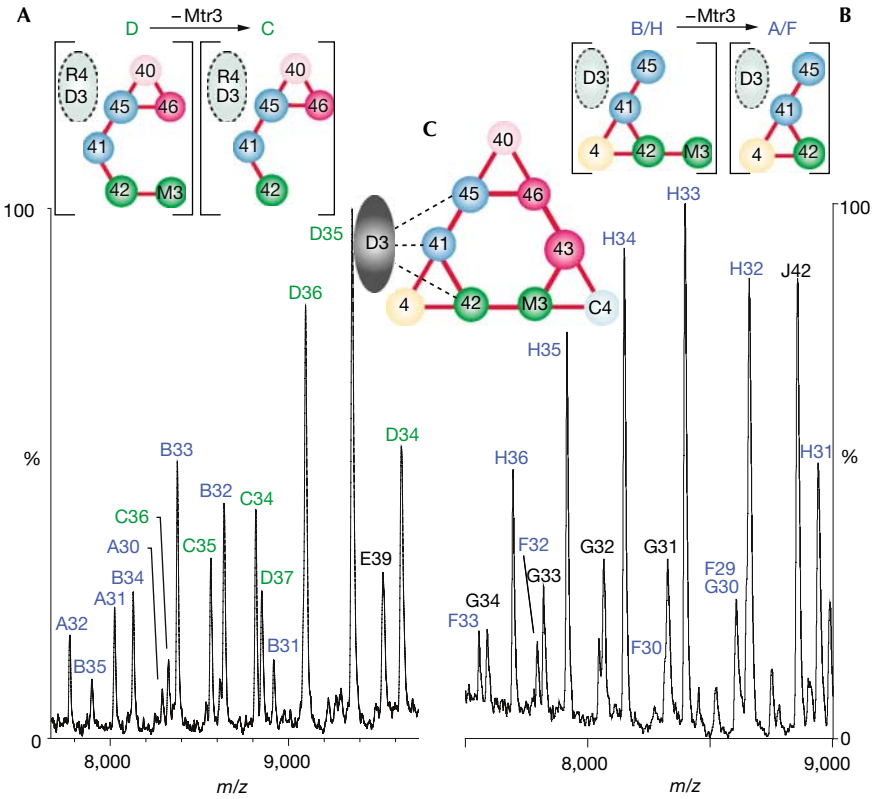

Fig 3 | Subcomplexes obtained after disruption of the exosome complexes in solution showing common dissociation pathways. (**A**) MS of Dis3-tagged exosome in 20% methanol. Charge states labelled in green are [exo-Csl4-Rrp43] and [exo-Csl4-Rrp43-Mtr3], series D (327 kDa) and C (299 kDa), respectively, where [exo] refers to the intact, ten-component complex, whereas those in blue are assigned as Rrp45:Rrp41:Rrp42:Rrp4:Dis3 with Mtr3 (series B, 276 kDa) and without Mtr3 (series A, 249 kDa). Charge state E39 is from [exo-Csl4]. (**B**) MS of Rrp41-tagged exosome in 33% dimethylsulphoxide. Charge states labelled in blue are Rrp45:Rrp41:Rrp4:Rrp42:Dis3 with Mtr3 (series H, 277 kDa) and without Mtr3 (series F, 249 kDa). Series G (258 kDa) is [exo-Csl4-Dis3] and J (371 kDa) is [exo-Csl4]. (**C**) Interaction map derived from MS data. The RNA-binding proteins Rrp40, Csl4 and Rrp4 each contact two ring dimers, whereas Dis3 contacts one or more proteins from the group Rrp45:Rrp41:Rrp42. MS, mass spectrometry.

simultaneously. The size of Dis3, together with the losses of RNA-binding proteins when Dis3 is present, suggests that interaction of Dis3 with the ring proteins is on the opposite face of the ring to Rrp40, Rrp4 and Csl4. The location of Dis3 completes our interaction map and enables us to construct a three-dimensional (3D) representation, with the RNA-binding proteins and Dis3 above and below the plane of the ring, respectively (Fig 4).

A common architecture for exosome complexes

It is relevant to assess our model in the light of other reports of protein–protein contacts for the yeast exosome. Low-resolution electron microscopy images of the yeast complex showed a ring arrangement, and an interaction map was proposed for the nine ring and peripheral proteins on the basis of sequence homology (Aloy *et al*, 2002). Strikingly, our MS data agree with only one contact in that model, Rrp45:Rrp40. In contrast, two-hybrid data for yeast, human and *Trypanosoma brucei* exosome interactions are generally in agreement with our model for the ring (Uetz *et al*, 2000; Ito *et al*, 2001; Oliveira *et al*, 2002; Raijmakers *et al*, 2002a,b; Estevez *et al*, 2003; Lehner & Sanderson, 2004). Furthermore, our data for the hexameric core arrangement are compatible with X-ray analysis of the exosome core from archaea, which showed a trimer of Rrp41-like/Rrp42-like dimers (Lorentzen *et al*, 2005). Sequence comparison linked archaeal Rrp41 with human/yeast Rrp41, Rrp46 and Mtr3 and archaeal Rrp42 with the remaining ring proteins, and the formation of Rrp45:Rrp41 and Rrp42:Mtr3 dimers in yeast was supported by coexpression data (Lorentzen *et al*, 2005). Recently, further X-ray structures of exosomes from archaea have been reported, which show the three peripheral proteins, all either AfuCsl4 or AfuRrp4, forming a cap on one face of the ring by binding adjacent Rrp41 and Rrp42 units from different Rrp41/Rrp42 dimers (Buttner *et al*, 2005) analogous to the bridging interactions deduced here. Our MS data, however, extend existing structural models to the more heterogeneous yeast exosome by providing strong evidence for the ring order of the six different proteins and allowing construction of a 3D representation in which the largest subunit, Dis3, and three different RNA-binding proteins are in contact with specific ring proteins.

It is interesting to consider our results in the light of established activities of the various subunits and their relative positions in our 3D model. The three RNA-binding proteins, above the ring in our model and in others, are likely to facilitate the size selection

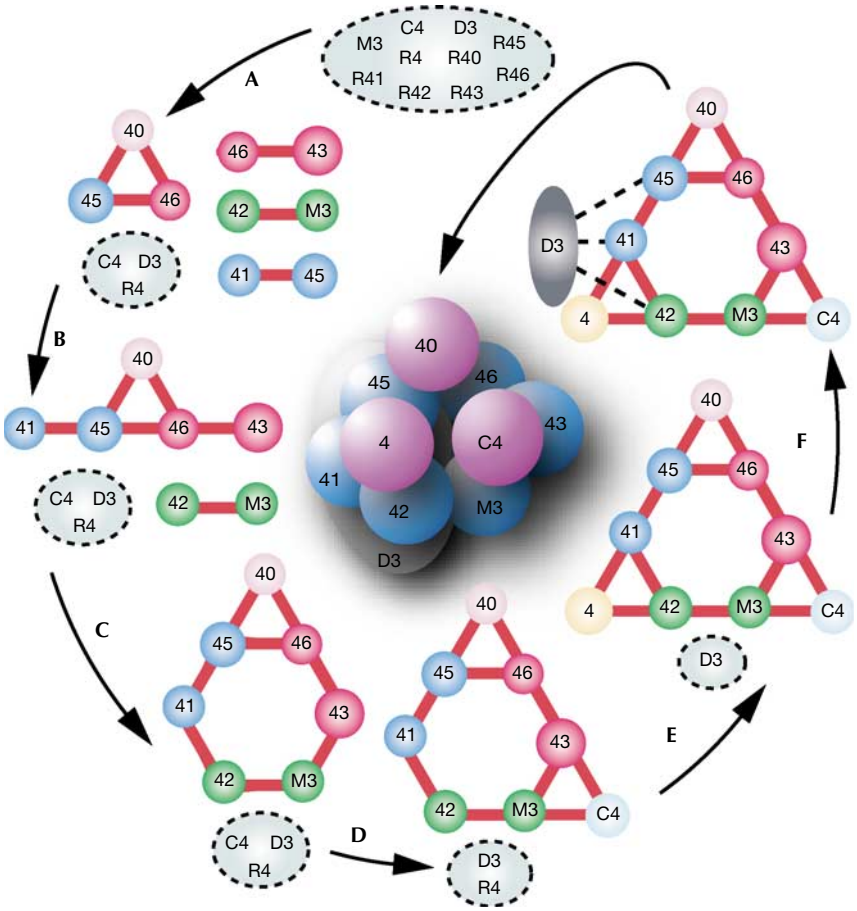

Fig 4 | Summary of the exosome subcomplexes and steps taken to build the 3D model. The ten-protein intact complex is shown in grey. Dotted lines indicate the subset of proteins the interactions of which are unknown at each step. Perturbation in solution was used to generate dimeric and trimeric complexes, confirmed by MS/MS (**A**), and overlap of these complexes is used to derive their subunit interactions (**B**). The loss of Mtr3 and Rrp43 orientates the Mtr3:Rrp42 dimer within the ring (**C**), and solution-phase loss of Rrp43, Mtr3 and Csl4 is used to locate Csl4 and Rrp4 (**D**,**E**). Analysis of subcomplexes containing Dis3 positions this protein in contact with Rrp45, Rrp41 and Rrp42 (**F**). Dis3 and (Csl4, Rrp40, Rrp4) are placed on opposite faces of the ring to construct the 3D model. 3D, three dimensional; MS, mass spectrometry.

and orientation of unstructured RNA substrates (Buttner *et al*, 2005; Lorentzen *et al*, 2005). So far, hydrolytic nuclease activity has been established only in Dis3 and Rrp4 (Mitchell *et al*, 1997; Estevez *et al*, 2001; Chekanova *et al*, 2002), whereas, of the six putative catalytic subunits in the ring of the yeast exosome, only Rrp41 has residues proposed to be essential for phosphorolytic activity (Lorentzen *et al*, 2005). The positioning of Dis3 in close proximity to Rrp41 in our model therefore raises the possibility that the hydrolytic and phosphorolytic exosome activities may well be concerted. More generally, with this approach we have highlighted new possibilities for MS of intact complexes, obtaining direct information on the structural organization of endogenous heterogeneous assemblies. We anticipate that interaction networks such as the one derived for the yeast exosome will prove invaluable, not only for constructing preliminary 3D models, as shown here, but also for the many hybrid structural and computational approaches in which individual subunits are fitted into low-resolution electron density maps (Russell *et al*, 2004).

METHODS

Complex isolation. Yeast strains, constructed according to published procedures (Rigaut *et al*, 1999; Puig *et al*, 2001), are listed in the supplementary information online.

The scavenger decapping and CBC complexes were purified using standard TAP protocols from 2 l of yeast culture (Rigaut *et al*, 1999; supplementary information online). After elution from the calmodulin column, samples were buffer exchanged to 1 M ammonium acetate using 500 µl Vivaspin (Sartorius Ltd, Epsom, Surrey, UK) or Nanosep (PALL Corp., Portsmouth, Hants, UK) centrifugal ultrafiltration devices.

Exosome complexes were purified from strains in which the Rrp6 gene was deleted to ensure that the cytoplasmic and not the Rrp6-containing nuclear form was obtained. We observed that the complex was relatively homogeneous after the first (IgG) purification step of the TAP procedure (supplementary Fig 1A online). Thus, after an initial standard TAP purification followed by buffer exchange using a 5 ml G25 column for Dis3 target protein, we used the following alternative protocol for all subsequent exosome

purification with 20 l of culture to increase the yield. Instead of batch purification, 1 ml IgG column chromatography was performed, followed by gel-filtration chromatography using a Superdex 200 column equilibrated with 400 mM ammonium acetate solution. After gel filtration, peak fractions were concentrated to about 3 μg/μl by ultrafiltration. Typical quantities of exosome complexes that were isolated were 200 μg from 20 l of yeast culture.

The TAP protocol is described fully at the following website: http://www-db.embl-heidelberg.de/ExternalInfo/seraphin/TAP.html.

Mass spectrometry. Nanoflow ESI data from the intact complexes were acquired as described previously (Sobott *et al*, 2002) using either an LCT MS or a modified QToF2 MS (Waters). Complexes were also confirmed by tryptic digestion and MS/MS (supplementary information online).

Supplementary information is available at *EMBO reports* online (http://www.emboreports.org).

ACKNOWLEDGEMENTS

We thank members of the Séraphin and Robinson labs as well as E. Conti and E. Lorenzen for fruitful discussions, S.L. Maslen for supporting MS/proteomics data, and S. Camier-Thuillier, M.G. McCammon and F. Sobott for critical reading of the manuscript. This work was supported by a Human Frontier Science Program (HSFP) grant (to C.V.R. and B.S.) and a Biotechnology and Biological Sciences Research Council (BBSRC) grant (to C.V.R. and H.H.), as well as by 'La ligue contre le Cancer' (Equipe Labelisée 2004) and the Agence Nationale de la Recherche (ANR) programme (to B.S). Authors' contributions: A.D., under the supervision of B.S., performed all complex selections and purifications; H.H., under the supervision of C.V.R., performed all MS analysis; H.H. and A.D., under the supervision of C.V.R. and B.S., built the exosome model; and T.T., under the supervision of C.V.R., compiled the software for determination of subcomplex composition (MolCalc) and the network algorithm. H.H., A.D., B.S. and C.V.R. wrote the paper.

REFERENCES

Aloy P, Ciccarelli FD, Leutwein C, Gavin AC, Superti-Furga G, Bork P, Bottcher B, Russell RB (2002) A complex prediction: three-dimensional model of the yeast exosome. *EMBO Rep* **3:** 628–635

Bushnell DA, Kornberg RD (2003) Complete, 12-subunit RNA polymerase II at 4.1-Å resolution: implications for the initiation of transcription. *Proc Natl Acad Sci USA* **100:** 6969–6973

Buttner K, Wenig K, Hopfner KP (2005) Structural framework for the mechanism of archaeal exosomes in RNA processing. *Mol Cell* **20:** 461–471

Chekanova JA, Dutko JA, Mian IS, Belostotsky DA (2002) *Arabidopsis thaliana* exosome subunit AtRrp4p is a hydrolytic 3′→5′ exonuclease containing S1 and KH RNA-binding domains. *Nucleic Acids Res* **30:** 695–700

Estevez AM, Kempf T, Clayton C (2001) The exosome of *Trypanosoma brucei*. *EMBO J* **20:** 3831–3839

Estevez AM, Lehner B, Sanderson CM, Ruppert T, Clayton C (2003) The roles of intersubunit interactions in exosome stability. *J Biol Chem* **278:** 34943–34951

Gavin AC *et al* (2002) Functional organization of the yeast proteome by systematic analysis of protein complexes. *Nature* **415:** 141–147

Gavin AC *et al* (2006) Proteome survey reveals modularity of the yeast cell machinery. *Nature* **440:** 631–636

Ghaemmaghami S, Huh WK, Bower K, Howson RW, Belle A, Dephoure N, O'Shea EK, Weissman JS (2003) Global analysis of protein expression in yeast. *Nature* **425:** 737–741

Gorlich D, Kraft R, Kostka S, Vogel F, Hartmann E, Laskey RA, Mattaj IW, Izaurraide E (1996) Importin provides a link between nuclear protein import and U snRNA export. *Cell* **87:** 21–32

Ito T, Chiba T, Ozawa R, Yoshida M, Hattori M, Sakaki Y (2001) A comprehensive two-hybrid analysis to explore the yeast protein interactome. *Proc Natl Acad Sci USA* **98:** 4569–4574

Lehner B, Sanderson CM (2004) A protein interaction framework for human mRNA degradation. *Genome Res* **14:** 1315–1323

Lewis JD, Gorlich D, Mattaj IW (1996) A yeast cap binding protein complex (yCBC) acts at an early step in pre-mRNA splicing. *Nucleic Acids Res* **24:** 3332–3336

Liu H, Rodgers ND, Jiao X, Kiledjian M (2002) The scavenger mRNA decapping enzyme DcpS is a member of the HIT family of pyrophosphatases. *EMBO J* **21:** 4699–4708

Lorentzen E, Walter P, Fribourg S, Evguenieva-Hackenberg E, Klug G, Conti E (2005) The archaeal exosome core is a hexameric ring structure with three catalytic subunits. *Nat Struct Mol Biol* **12:** 575–581

Malys N, Carroll K, Miyan J, Tollervey D, McCarthy JE (2004) The 'scavenger' m7GpppX pyrophosphatase activity of Dcs1 modulates nutrient-induced responses in yeast. *Nucleic Acids Res* **32:** 3590–3600

Mazza C, Segref A, Mattaj IW, Cusack S (2002) Large-scale induced fit recognition of an m^7 GpppG cap analogue by the human nuclear cap-binding complex. *EMBO J* **21:** 5548–5557

Mitchell P, Tollervey D (2000) Musing on the structural organization of the exosome complex. *Nat Struct Biol* **7:** 843–846

Mitchell P, Petfalski E, Shevchenko A, Mann M, Tollervey D (1997) The exosome: a conserved eukaryotic RNA processing complex containing multiple 3′→5′ exoribonucleases. *Cell* **91:** 457–466

Oliveira CC, Gonzales FA, Zanchin NI (2002) Temperature-sensitive mutants of the exosome subunit Rrp43p show a deficiency in mRNA degradation and no longer interact with the exosome. *Nucleic Acids Res* **30:** 4186–4198

Puig O, Caspary F, Rigaut G, Rutz B, Bouveret E, Bragado-Nilsson E, Wilm M, Seraphin B (2001) The tandem affinity purification (TAP) method: a general procedure of protein complex purification. *Methods* **24:** 218–229

Raijmakers R, Egberts WV, van Venrooij WJ, Pruijn GJ (2002a) Protein–protein interactions between human exosome components support the assembly of RNase PH-type subunits into a six-membered PNPase-like ring. *J Mol Biol* **323:** 653–663

Raijmakers R, Noordman YE, van Venrooij WJ, Pruijn GJ (2002b) Protein–protein interactions of hCsl4p with other human exosome subunits. *J Mol Biol* **315:** 809–818

Rigaut G, Shevchenko A, Rutz B, Wilm M, Mann M, Seraphin B (1999) A generic protein purification method for protein complex characterization and proteome exploration. *Nat Biotechnol* **17:** 1030–1032

Russell RB, Alber F, Aloy P, Davis FP, Korkin D, Pichaud M, Topf M, Sali A (2004) A structural perspective on protein–protein interactions. *Curr Opin Struct Biol* **14:** 313–324

Sobott F, Robinson CV (2002) Protein complexes gain momentum. *Curr Opin Struct Biol* **12:** 729–734

Sobott F, Hernandez H, McCammon MG, Tito MA, Robinson CV (2002) A tandem mass spectrometer for improved transmission and analysis of large macromolecular assemblies. *Anal Chem* **74:** 1402–1407

Symmons MF, Williams MG, Luisi BF, Jones GH, Carpousis AJ (2002) Running rings around RNA: a superfamily of phosphate-dependent RNases. *Trends Biochem Sci* **27:** 11–18

Uetz P *et al* (2000) A comprehensive analysis of protein–protein interactions in *Saccharomyces cerevisiae*. *Nature* **403:** 623–627

Wang Z, Kiledjian M (2001) Functional link between the mammalian exosome and mRNA decapping. *Cell* **107:** 751–762